Cell Reports, Volume *35*

Supplemental information

ELAVL1 primarily couples mRNA stability with the 3′ UTRs of interferon-stimulated genes

Katherine Rothamel, Sarah Arcos, Byungil Kim, Clara Reasoner, Samantha Lisy, Neelanjan Mukherjee, and Manuel Ascano

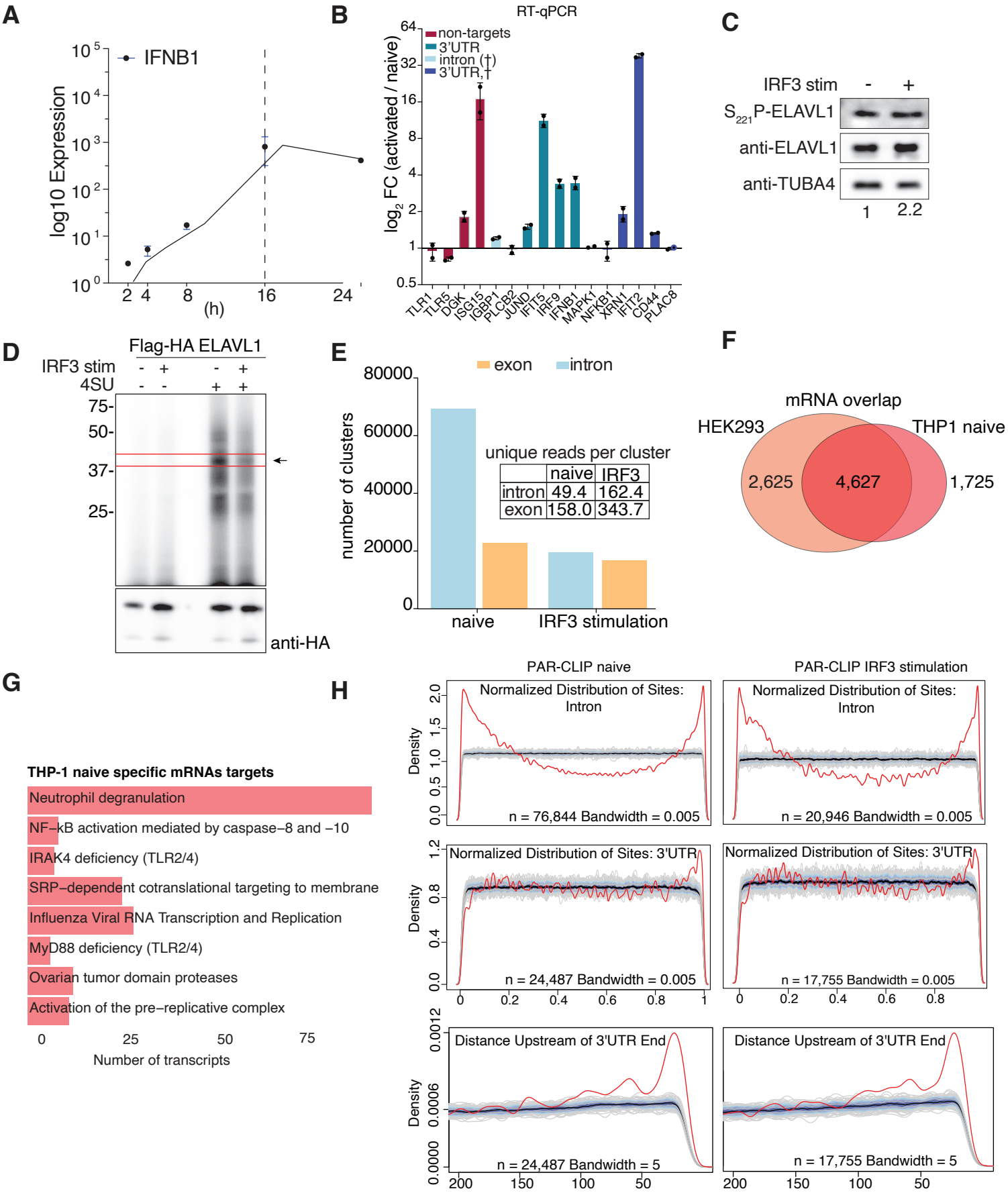
A
IFNB1
log10 Expression
(h)
B
RT-qPCR
non-targets
3'UTR
intron (†)
3'UTR,†
log2 FC (activated / naive)
TLR1 TLR5 DGK ISG15 IGBP1 PLCB2 JUND IFIT5 IRF9 IFNB1 MAPK1 NFKB1 XRN1 IFIT2 CD44 PLAC8
C
IRF3 stim
S221P-ELAVL1
anti-ELAVL1
anti-TUBA4
D
Flag-HA ELAVL1
IRF3 stim
4SU
anti-HA
E
exon
intron
number of clusters
unique reads per cluster
naive IRF3
intron 49.4 162.4
exon 158.0 343.7
naive
IRF3 stimulation
F
mRNA overlap
HEK293
THP1 naive
2,625
4,627
1,725
G
THP-1 naive specific mRNAs targets
Neutrophil degranulation
NF−kB activation mediated by caspase−8 and −10
IRAK4 deficiency (TLR2/4)
SRP−dependent cotranslational targeting to membrane
Influenza Viral RNA Transcription and Replication
MyD88 deficiency (TLR2/4)
Ovarian tumor domain proteases
Activation of the pre−replicative complex
Number of transcripts
H
PAR-CLIP naive
PAR-CLIP IRF3 stimulation
Normalized Distribution of Sites: Intron
n = 76,844 Bandwidth = 0.005
n = 20,946 Bandwidth = 0.005
Normalized Distribution of Sites: 3'UTR
n = 24,487 Bandwidth = 0.005
n = 17,755 Bandwidth = 0.005
Distance Upstream of 3'UTR End
n = 24,487 Bandwidth = 5
n = 17,755 Bandwidth = 5
Density

Supplemental Figure 1: PAR-CLIP identifies and maps the cell-type-specific and condition-specific binding sites of ELAVL1, Related to Figure 1

(**A**). THP-1 cells were stimulated with the STING agonist cGAMP (EC50), and RNA was collected at indicated time points. RT-qPCR was used to measure the mRNA levels of *IFNB1.* (**B**) Bar graph of the log_2 foldchange of mRNA levels (RT-qPCR) in immune activated cells compared to naive. (**C**) Immunoblot shows the whole-cell amount of phosphoserine (S221) ELAVL1 and ELAVL1 in both naive and immune activated cells. (**D**) Phosphoimage showing both the non-crosslinked (no 4SU) and crosslinked ELAVL1 to RNA samples of the IP for PAR-CLIP. Immunoblot shows that equal amounts of immunoprecipitated ELAVL1 from each condition. (**E**) Bar graph showing the number of clusters that mapped either to exons and introns across the two cellular conditions. Inset shows the average number of unique reads for each exonic- or intronic- cluster across the cellular states. (**F**) Venn diagram showing the overlap of target mRNAs from HEK293 (Mukherjee et al. 2011) and THP-1 naïve. (**G**) Reactome pathway analysis for the mRNAs that were uniquely bound in THP-1 cells compared to HEK293. (**H**) Metagene analysis showing the normalized distribution of binding sites across introns or the 3'UTR across both conditions.

A

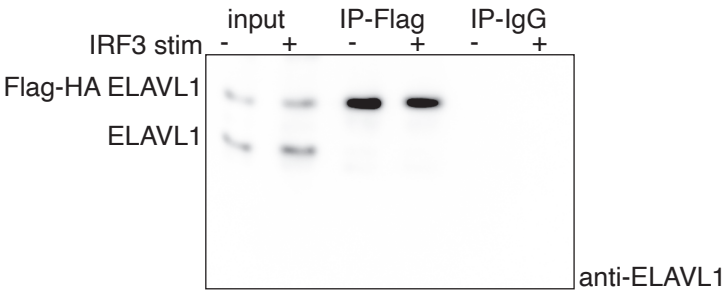
input
IP-Flag
IP-IgG
IRF3 stim - + - + - +
Flag-HA ELAVL1
ELAVL1
anti-ELAVL1

B

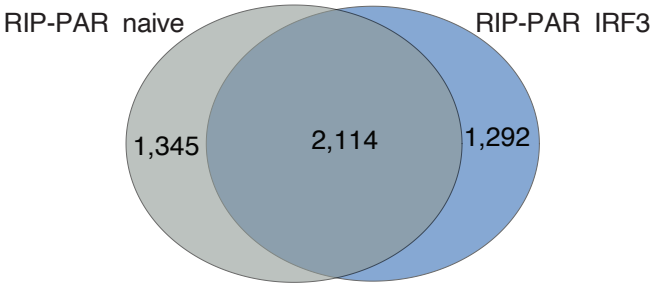
RIP-PAR naive
RIP-PAR IRF3
1,345
2,114
1,292

C

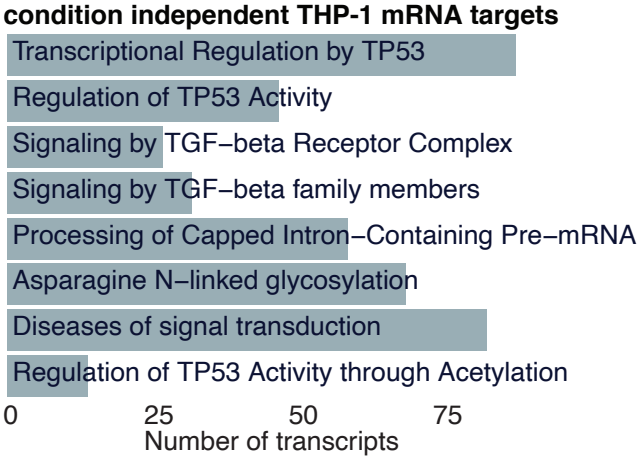
condition independent THP-1 mRNA targets
Transcriptional Regulation by TP53
Regulation of TP53 Activity
Signaling by TGF–beta Receptor Complex
Signaling by TGF–beta family members
Processing of Capped Intron–Containing Pre–mRNA
Asparagine N–linked glycosylation
Diseases of signal transduction
Regulation of TP53 Activity through Acetylation
0
25
50
75
Number of transcripts

D

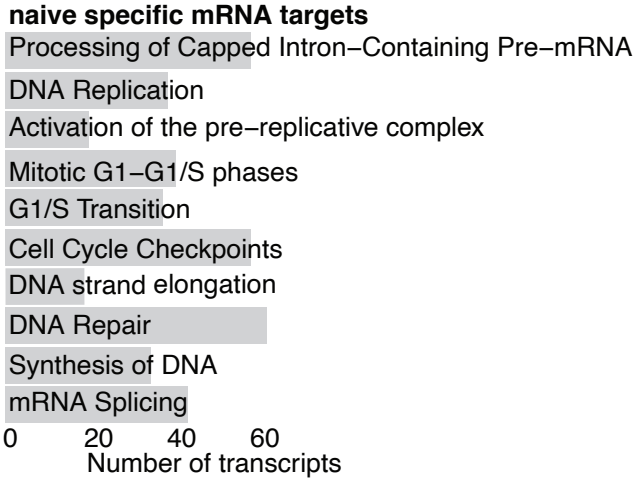
naive specific mRNA targets
Processing of Capped Intron–Containing Pre–mRNA
DNA Replication
Activation of the pre–replicative complex
Mitotic G1–G1/S phases
G1/S Transition
Cell Cycle Checkpoints
DNA strand elongation
DNA Repair
Synthesis of DNA
mRNA Splicing
0
20
40
60
Number of transcripts

E

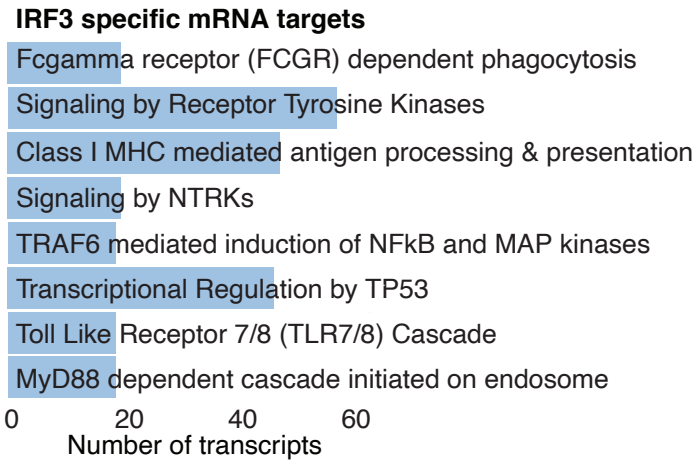
IRF3 specific mRNA targets
Fcgamma receptor (FCGR) dependent phagocytosis
Signaling by Receptor Tyrosine Kinases
Class I MHC mediated antigen processing & presentation
Signaling by NTRKs
TRAF6 mediated induction of NFkB and MAP kinases
Transcriptional Regulation by TP53
Toll Like Receptor 7/8 (TLR7/8) Cascade
MyD88 dependent cascade initiated on endosome
0
20
40
60
Number of transcripts

Supplemental Figure 2: PAR-CLIP and RIP-Seq identify enriched transcripts that are condition independent or dependent , Related to Figure 2

(**A**) ELAVL1 immunoblot from an IP (anti-Flag) of Flag-HA ELAVL1 in naïve and immune activated THP-1 cells. (**B**) Venn diagram showing the overlap between the bound (PAR-CLIP) and enriched (RIP-Seq) mRNA transcripts across conditions. (**C**) Bar graph of a Reactome pathway analysis for each group of transcripts that were either shared (from S2A) between the two conditions or unique bound and enriched in the naïve (**D**) or (**E**) the stimulated states.

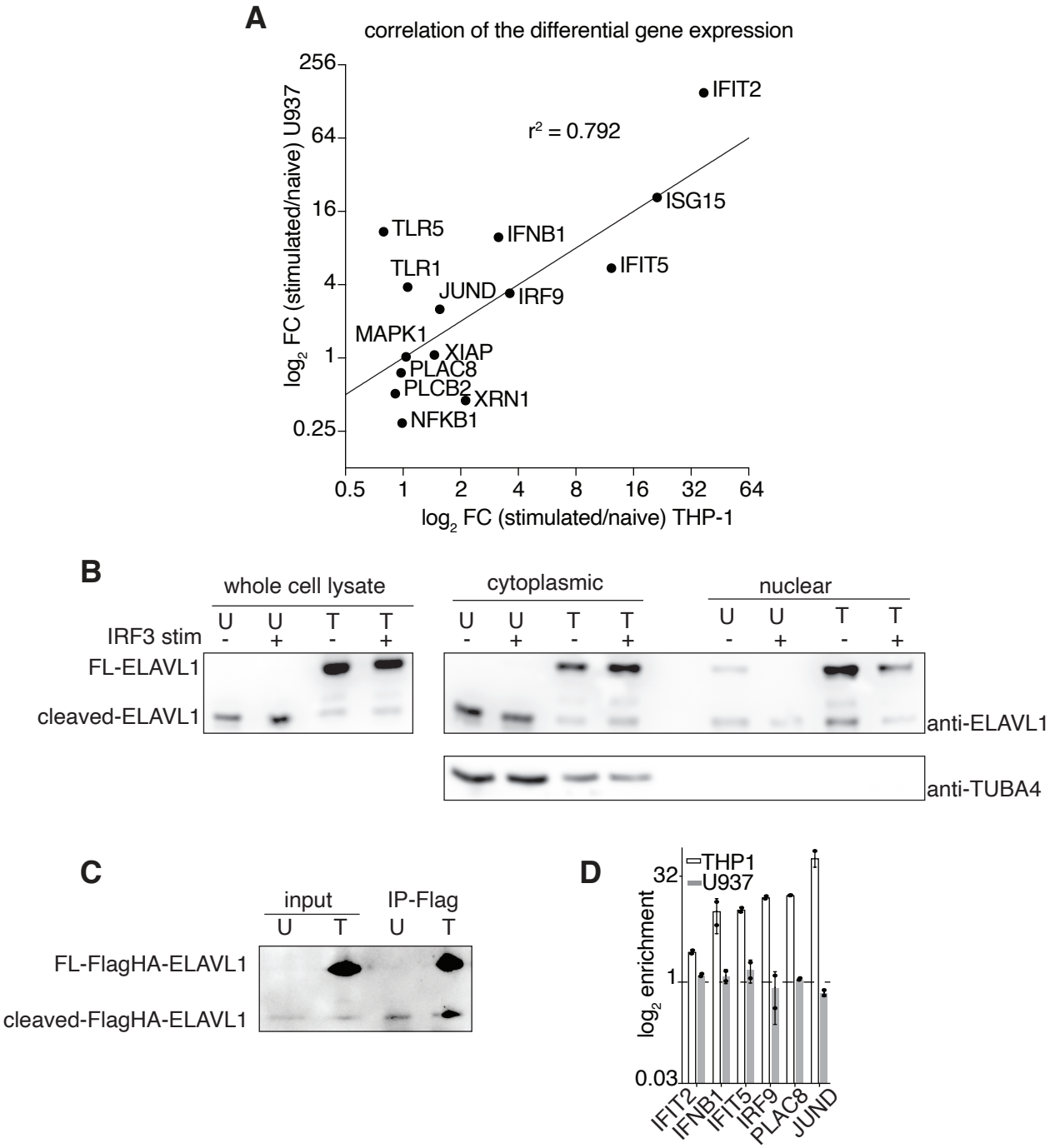
A
correlation of the differential gene expression
log2 FC (stimulated/naive) U937
log2 FC (stimulated/naive) THP-1
r2 = 0.792
IFIT2
ISG15
TLR5
IFNB1
TLR1
IFIT5
JUND
IRF9
MAPK1
XIAP
PLAC8
PLCB2
XRN1
NFKB1
256
64
16
4
1
0.25
0.5
1
2
4
8
16
32
64
B
whole cell lysate
cytoplasmic
nuclear
IRF3 stim
U U T T
- + - +
FL-ELAVL1
cleaved-ELAVL1
anti-ELAVL1
anti-TUBA4
C
input
IP-Flag
U T U T
FL-FlagHA-ELAVL1
cleaved-FlagHA-ELAVL1
D
THP1
U937
log2 enrichment
32
1
0.03
IFIT2
IFNB1
IFIT5
IRF9
PLAC8
JUND

Supplemental Figure 3: ELAVL1 in U973 cells is predominantly cleaved, Related to Figure 4

(A) Correlation plot of gene expression foldchanges (activated /naïve) of the stated ISG transcripts between THP-1 and U937 cells. (**B**) Immunoblot against endogenous ELAVL1 on biochemically fractionated lysates in naïve and immune activated U937 (U) and THP-1 cells (T). The predominant form of ELAVL1 is a truncated form that is ~24 kDa, independent of the cellular state. (**C**) Anti-HA immunoblot from the input and IP (anti-Flag) of Flag-Ha ELAVL1 in U937 (U) and THP-1 cells (T). Based on molecular weight, the exogenous form of Flag-HA ELAVL1 appears cleaved in U937 compared to THP-1.(**D**) Bar graph comparing the RIP RT-qPCR enrichment levels of ISG transcripts in U937 cells and THP-1 cells. The transcripts were chosen because they were validated, highly enriched targets in THP-1 cells.

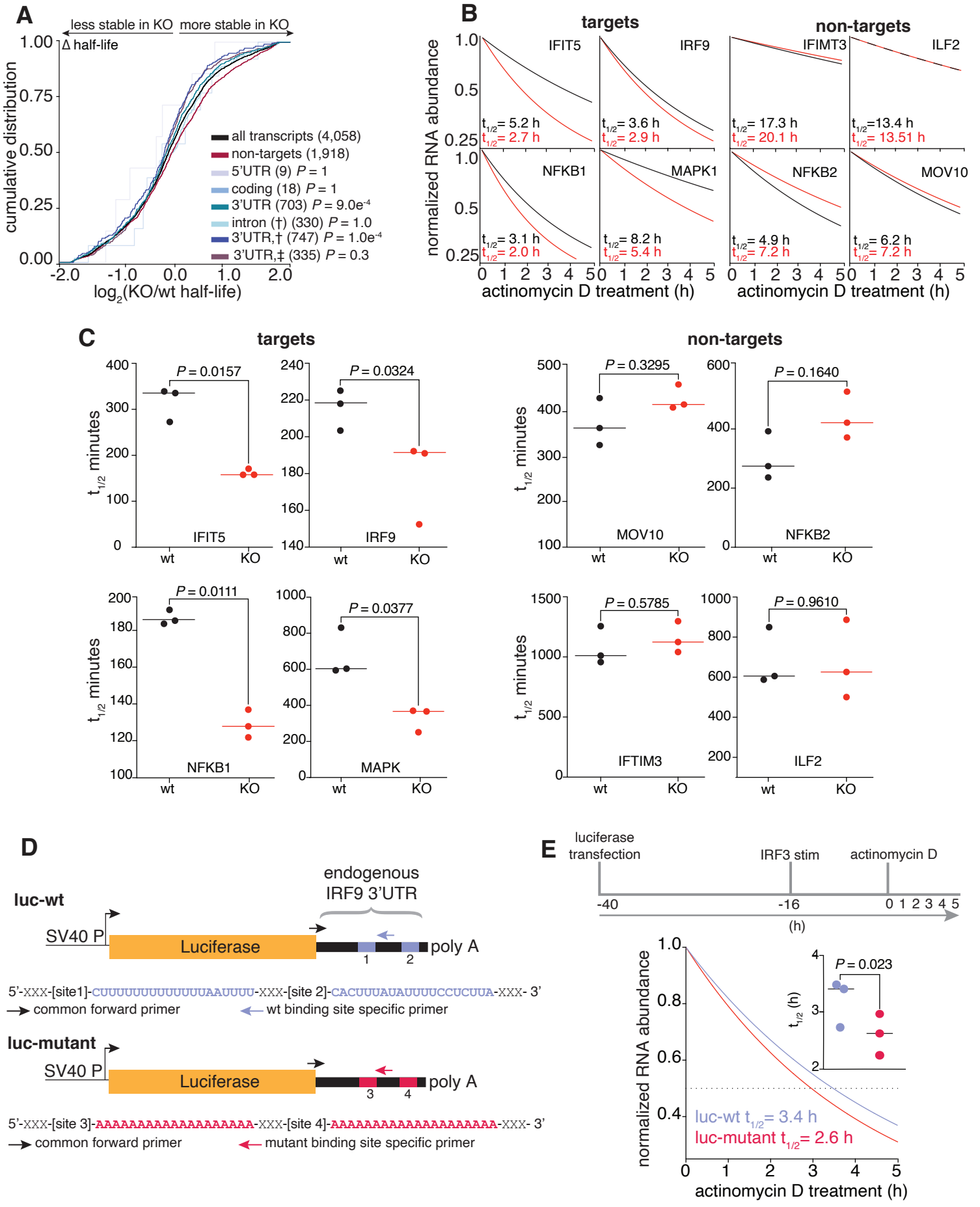
A
less stable in KO
more stable in KO
Δ half-life
cumulative distribution
log2(KO/wt half-life)
all transcripts (4,058)
non-targets (1,918)
5'UTR (9) P = 1
coding (18) P = 1
3'UTR (703) P = 9.0e-4
intron (†) (330) P = 1.0
3'UTR,† (747) P = 1.0e-4
3'UTR,‡ (335) P = 0.3
B
targets
non-targets
IFIT5
IRF9
IFIMT3
ILF2
NFKB1
MAPK1
NFKB2
MOV10
normalized RNA abundance
actinomycin D treatment (h)
C
targets
non-targets
t1/2 minutes
P = 0.0157
P = 0.0324
P = 0.3295
P = 0.1640
P = 0.0111
P = 0.0377
P = 0.5785
P = 0.9610
IFIT5
IRF9
MOV10
NFKB2
NFKB1
MAPK
IFTIM3
ILF2
wt
KO
D
luc-wt
endogenous IRF9 3'UTR
SV40 P
Luciferase
poly A
5'-XXX-[site1]-CUUUUUUUUUUUUUAAUUUU-XXX-[site 2]-CACUUUAUAUUUUCCUCUUA-XXX- 3'
common forward primer
wt binding site specific primer
luc-mutant
5'-XXX-[site 3]-AAAAAAAAAAAAAAAAAAA-XXX-[site 4]-AAAAAAAAAAAAAAAAAAAA-XXX- 3'
mutant binding site specific primer
E
luciferase transfection
IRF3 stim
actinomycin D
(h)
normalized RNA abundance
actinomycin D treatment (h)
P = 0.023
luc-wt t1/2 = 3.4 h
luc-mutant t1/2 = 2.6 h

Supplemental Figure 4: KO determines transcripts whose half-lives are dependent on the presence of ELAVL1, Related to Figure 6

(**A**) Cumulative distribution plot of the $\log_2$ foldchange (KO/wt) in half-life showing the group of transcripts whose half-lives are most affected by the loss of ELAVL1. (**B**) The calculated RNA half-lives and stability plots of transcripts indicated. RNA half-lives were measured using actinomycin D and RT-qPCR. (**C**) Pairwise comparisons of the RNA half-lives in the presence or absence of ELAVL1 for either non-target or target transcripts. (**D**) To test if an exogenous transcript can be stabilized in an ELAVL1 site-dependent manner, we constructed two gene reporters from the luciferase ORF and wt *IRF9* 3'UTR or mutant *IRF9* 3'UTR. Schematic shows luciferase ORF with either the wt *IRF9* 3'UTR or the mutant. (**E**) Schematic of luciferase reporter experiment. RNA-stability profiles and a pairwise comparison of the half-lives of an exogenous gene (ORF of luciferase) expressed with either the wt or mutant 3'UTR *IRF9.*

SUPPLEMENTAL FIGURE LEGENDS

Supplemental Figure 1. PAR-CLIP identifies and maps the cell-type-specific and condition-specific binding sites of ELAVL1, Related to Figure 1

Supplemental Figure 2. PAR-CLIP and RIP-Seq identify enriched transcripts that are condition independent or dependent, Related to Figure 2

Supplemental Figure 3. ELAVL1 in U973 cells is predominantly cleaved, Related to Figure to Figure 4

Supplemental Figure 4. KO determines transcripts whose half-lives are dependent on the presence of ELAVL1, Related to Figure 6

SUPPLEMENTAL TABLE LEGENDS

Table S1. RNA-Seq counts table and DeSeq2 differential expression table comparing stimulated and naïve THP-1 gene expression, Related to Figure 1

Table S2. Summary table for PARalyzer output, Related to Figure 1

Table S3. Transcript level table with combined RIP-Seq, RNA-Seq and PAR-CLIP datasets, Related to Figure 2

Table S4. Cluster level tables with combined RIP-Seq, RNA-Seq and PAR-CLIP data, Related to Figure 2

Table S5. Reactome pathway analysis of condition dependent and independent enriched targets of THP-1, Related to Figure 3

Table S6. SLAM-Seq half-life data, Related to Figure 5

Table S7. Reactome pathway analysis of the functional targets of ELAVL1, Related to Figure 7

Table S8. The Primers and guide RNAs Used in this Study, Related to the STAR Methods